ACTA STEREOL 1999; 18/3: 427-434
ORIGINAL SCIENTIFIC PAPER

CONVEX HULLS IN Z^2: APPLICATION TO CELL SORTING

Christophe BOUDRY [1,2,3], Michel COSTER[1], Liliane CHERMANT[1], Paulette HERLIN[2], Jean-Louis CHERMANT[1]

1: LERMAT, UPRESA CNRS 6004, ISMRA, 6 Bld Maréchal Juin, 14050 Caen Cedex, France
2: Centre F. Baclesse, Service d'Anatomie Pathologique (Cytométrie en Images) 14076 Caen Cedex 5, France
3: Laboratoire de Neurosciences, UMR CNRS 6551, Université de Caen, Caen, France

ABSTRACT

The aim of this paper is to evaluate the influence of the image frame and the influence of the number of orientations used in this frame on the characterisation of damaged nuclei and aggregates for image cytometry DNA ploidy measurements.

Key words : convex hull, DNA ploidy measurement, solid tumor.

INTRODUCTION

Fully automatic DNA ploidy measurements of tumors, using image cytometry requires the elimination of debris and aggregates, which are generated during sample preparation (Boudry, 1997). Among these debris, two categories can be distinguished, according to their shape: nuclei damaged during the dissociation of tissue and aggregates, mainly generated during the sedimentation of nuclei on glass slides. These debris and aggregates are characterised by concavities while undamaged nuclei are mainly convex.
A way to analyse concavity is to measure parameters on objects and to compare the results to those obtained on the convex hull of the same objects. Two parameters can be available: perimeter and surface area but surface area is less sensitive to noise than perimeter (Coster and Chermant, 1989). Concavity can be then expressed as the ratio between initial surface area of object and surface area of the convex hull of the object (Ai/Ac). Several convex hulls (CH) can be defined in the digital space. The most popular one is the polygonal convex hull, which connects the convex points of the digitised perimeter of objects. Other convex hulls can be defined referring to primary or secondary directions of the chosen grid. They are computed thanks to parallel algorithms, using thickening morphological operators (Serra, 1982; Coster and Chermant, 1985, 1989). In these conditions, three convex hulls can be defined for the square grid: hexadecagonal (16 sides), octogonal (8 sides), square (4 sides) and two for the hexagonal grid: dodecagonal (12 sides) and hexagonal (6 sides). Consequently, as much ratio Ai/Ac can be computed (5).

The aim of this present paper is to propose two algorithms for hexadecagonal and dodecagonal convex hull building, using structuring elements of size one (instead of the classically used structuring elements of size two), (Serra, 1988). The work will focus on the ability of the different ratio Ai/Ac obtained, to characterise damaged nuclei and aggregates.

MATERIAL AND INSTRUMENTATION

Biological material and image cytometry

The study was performed on an archival brain tumour (astrocytoma grade 2) prepared according to Van-Driel Kulker et al. (1987) and DNA stained according to Feulgen and Rossenbeck (1924) as described previously (Duigou et al., 1997).
The image cytometer consists of a BH2 Olympus microscope, a scanning stage, a matrox PIP 1024 frame grabber and a Sony CCD camera. Images were acquired using systematic sampling. Integrated optical density measurements were done at a resolution of 512×512 pixels in 8 bits (1 pixel=0.11μm^2). Fifty images representing 1079 elements were studied (example shown in Figure 1).

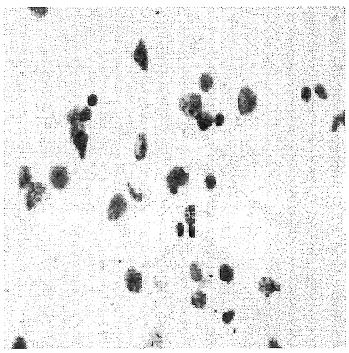

Figure 1: Example of an image.

Segmented events were interactively classified as undamaged nuclei on one hand, damaged nuclei and aggregates on the other hand, assuming that it corresponds to the reference sorting .

Performances of characterisation of damaged nuclei and aggregates

The ability of each Ai/Ac to characterise damaged nuclei and aggregates obtained with the six types of convex hull was evaluated. In order to perform a comprehensive comparison, for each Ai/Ac, sensitivities (S) were computed, corresponding to a percentage of false positive (FP) equal to 10%. S is defined as the percentage of damaged nuclei and aggregates correctly classified by reference to interactive sorting. False positive rate (FP) is defined as the percentage of undamaged nuclei misclassified as damaged nuclei or aggregates.

METHOD DEVELOPED

Hexadecagonal and dodecagonal convex hull building

Octogonal, square and hexagonal convex hulls can be computed by thickening, using size one structuring elements. These convex hulls are obtained considering primary directions of the frame. Two alternatives exist to compute convex hulls using secondary directions (hexadecagonal and dodecagonal convex hull). The first one is to use thickening morphological operators, with size two structuring elements (Serra, 1988). This possibility

requires imaging softwares offering the ability to use size two structuring elements; such softwares were not available in the laboratory. The second possibility is to start from octogonal and hexagonal convex hull obtained, considering primary directions, and to perform thinning in order to reach respectively hexadecagonal and dodecagonal convex hulls. This last solution was chosen. This is based on the following relationship:

$$CH(X) \subset CHn(X) \subset CHm(X) \subset X$$

where C(X) represents the Euclidean or polygonal convex hull of the object X; CHn(X) and CHm(X) represent convex hulls of the object X, using n and m orientations in the frame (with n>m). It means that a convex hull of an object X, obtained using n orientations, is fully included in the convex hull of the same object, using m orientations, if n is superior to m. It is then theoretically possible to obtain by thinning the hexadecagonal convex hull from octogonal convex hull and the dodecagonal convex hull from the hexagonal one, using a structuring element of size one.
As for example, algorithm developed for the computation of dodecagonal convex hull is presented in Figure 2.

Table 1: Structuring element used to obtain by thinning, hexadecagonal and dodecagonal convex hull from octogonal and hexagonal convex hull, respectively.

a	B
0 0 0 1 1 1 1	0 0 0 0 1 1 1 1 1

The algorithm developed starts by the computation of hexagonal convex hull. For each rotation of the structuring element (presented in Table 1a), successive size one thinnings are performed from the hexagonal convex hull. The algorithm is mainly based on the condition that, for a given rotation of the structuring element and for each object, thinning stops when it hits initial objects.

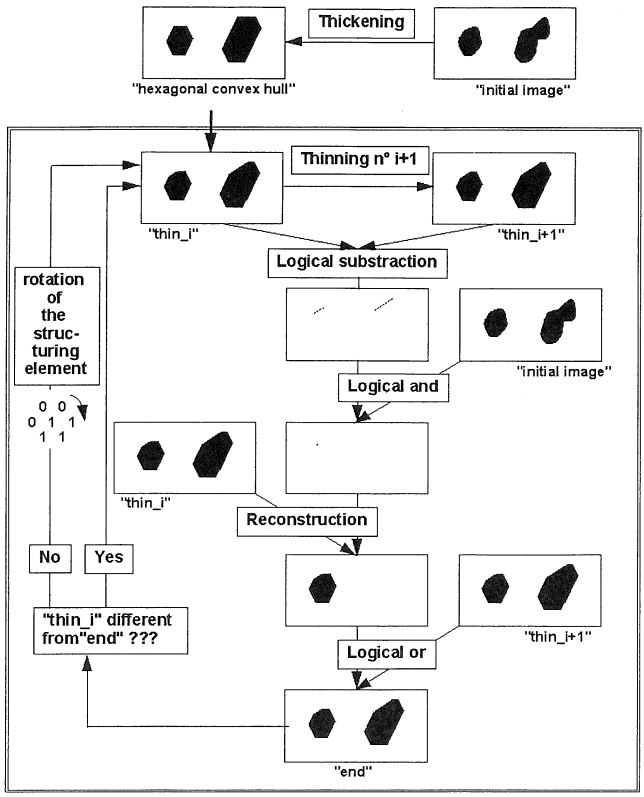

Figure 2: Algorithm developed for the computation of dodecagonal convex hull.

Furthermore, the progress to the next rotation of the structuring element, is done when all the objects are hit by thinning. The control is obtain by two successive logical operations (*substraction* and *and*); if the object is hit, the resulting image contains a marker which allows the reconstruction of the object at the state *i* (Figure 2).
A logical *or* allows to recover on the reconstructed image then other objects (state *i+1*), which have not been yet hit. When all the objects are hit by thinning, the rotation of the structuring element can take place. It must be noticed that this algorithm is fully parallel, avoiding individual treatments, objects per objects. It is then independent on the number of objects per images. Algorithm developed for the computation of hexadecagonal convex hull is built exactly on the same scheme. The structuring element used is presented in Table 1b and the number of possible orientations is 8 instead of 6 for dodecagonal convex hull building.

RESULTS

The values of the different Ai/Ac ratios for the population of the astrocytoma grade 2 was assessed (n=1079), (Figure 3). Values of Ai/Ac ratio decrease from polygonal convex hull to square convex while standard deviation rise.

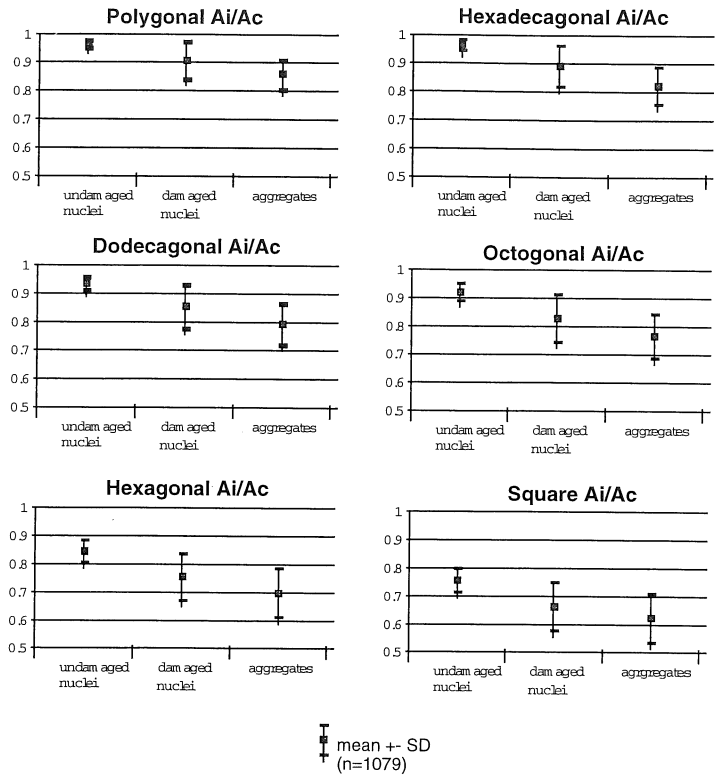

Figure 3: Values of the several ratios Ai/Ac for undamaged nuclei, damaged nuclei and aggregates for the population of astrocytoma grade 2.

The correlation coefficient of the various Ai/Ac ratios to polygonal Ai/Ac ratio were calculated for the same population. Correlation coefficient decrease from hexadecagonal convex hull to square convex hull (Table 2) suggesting a loss of precision for the calculation of Ai/Ac ratio.

Table 2: Correlation coefficient of the different Ai/Ac ratios as compared to polygonal Ai/Ac ratio.

Ai/Ac	Polygonal	Hexa-decagonal	Dode-cagonal	Octogonal	Hexagonal	Square
Correlation coefficient	1	0.94	0.91	0.88	0.8	0.76

The ability of the several Ai/Ac ratios to characterise damaged nuclei and aggregates was evaluated (Table 3). The percentage of damaged nuclei and aggregates well classified decreases from polygonal convex hull to square convex hull, confirming the loss of precision on the computation of Ai/Ac ratio.

Table 3: Characterisation of aggregates and damaged nuclei using the several Ai/Ac ratios.

Ai/Ac	Polygonal	Hexa-decagonal	Dode-cagonal	Octogonal	Hexagonal	Square
S aggregates (%)	92	92	87	76	71	55
S damaged nuclei (%)	53	41	39	35	34	28
FP (%)	10	10	10	10	10	10

INTERPRETATION OF RESULTS THANKS TO THEORETICAL OBJECTS

The previous experimentation showed that the values of Ai/Ac ratios decrease while the number of orientations used for the computation of convex hulls decrease.

convex hull	Polygonal	Hexadeca-gonal	Dodeca-gonal	Octogonal	Hexagonal	Square
Ac	16748	16952	17131	17179	18339	20878
Ai/Ac	86.58	85.52	84.65	84.41	79.07	69.46

Figure 4: Example of the evolution of Ai/Ac ratio for a given object.

The theoretical example presented in Figure 4 explains that this is due to the increase of the surface area of the convex hull when considering polygonal to square convex hulls. This example does not explain the loss of precision observed. An explanation of this loss of precision can be searched in the orientation and lengthening of the studied objects. Apart from polygonal convex hull, the surface area of hexadecagonal, dodecagonal, octogonal hexagonal and square convex hulls is dependent on the orientation of object. The theoretical example presented in Figure 5 shows that the extent of variation of surface area rise when the number of orientations used decrease. Values obtained for Ai/Ac ratio, according to the orientation of a given object, fluctuate only between orientations of the convex hull. For the square convex hull, only 4 orientations are used and values of Ai/Ac ratio widely fluctuate between these 4 orientations in a periodic mode. On the contrary, for hexadecagonal convex hull, 16 orientations are used and values of Ai/Ac obtained, while the object rotates, do not vary significantly between these orientations.

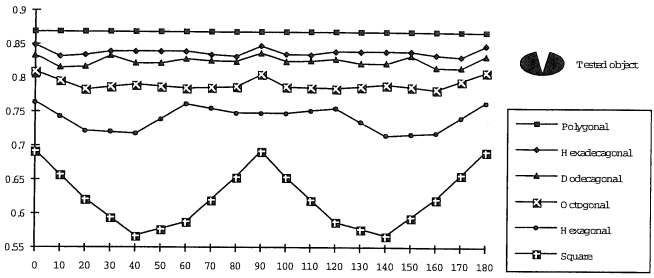

Figure 5: Example of the evolution of Ai/Ac ratios as a function of orientation (from 0° to 180°) for a given object.

Variations of Ai/Ac values between two orientations for each convex hull (corresponding to the period: 22.5° for hexadecagonal convex hull, 30° for dodecagonal convex hull, 45° for octogonal convex hull, 60° for hexagonal convex hull and 90° for square convex hull) are presented in Figure 6. There are not any variation when considering Ai/Ac ratio obtained with polygonal convex hull whereas obvious variations exist for the other Ai/Ac ratios. These variations rise when the number of orientation of the convex hull decrease.

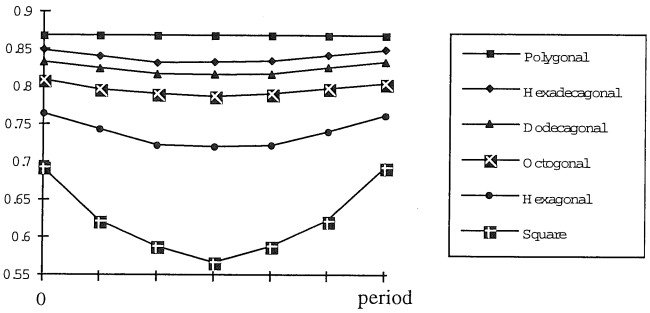

Figure 6: Example of the evolution of Ai/Ac ratio as a function of orientation (inside the period of each convex hull) for the same object presented in Figure 4.

A theoretical example presented in Figure 7 illustrates that the influence of the orientation on the precision of Ai/Ac values rises with the lengthening of objects.

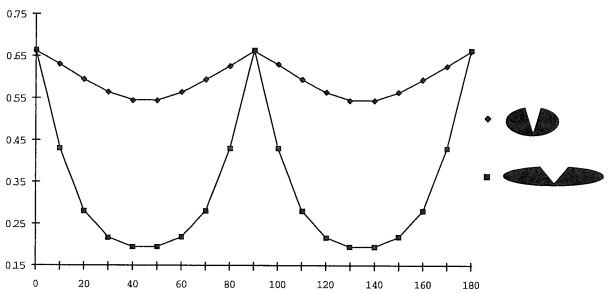

Figure 7: Example of the evolution of Ai/Ac ratio obtained from square convex hull for two lengthened objects (having the same Ai/Ac ratio obtained from polygonal convex hull).

This figure shows an example of Ai/Ac ratio obtained from square convex hull for two objects which differs only by their lengthening) that the error done is as much large as the object is lengthened (the two objects have strictly the same Ai/Ac obtained from polygonal convex hull, equal to 0.87).

The loss of precision on the computation of Ai/Ac ratio is due to the variation of orientation and lengthening of objects. This loss of precision is as much important as the number of orientations used is low.

CONCLUSION

The choice of the image frame (square or hexagonal lattice) and the number of orientations used in this frame have a great influence on the characterisation of damaged nuclei and aggregates. When considering the importance of a correct elimination of aggregates, this choice is very critic for the quality of DNA ploidy measurements.
If the use of polygonal convex hull leads to the best characterisation of undamaged nuclei and aggregates, its computation requires individual analysis, which could penalise time treatment. On the contrary, Ai/Ac ratio based on hexadecagonal and dodecagonal convex hull can be used for damaged nuclei and aggregates characterisation while accepting a minimum loss of precision. This choice offers the ability to obtain computation independently on the number of objects of the image, allowing time saving.
As a conclusion and referring to the example developed in this paper, the chosen image frame and the number of orientations used for the calculation of any parameter must be carefully chosen to solve biological problems, using image analysis.

ACKNOWLEDGMENTS

This work was done under the auspices of "**Pôle Traitement et Analyse d'Images** de Basse-Normandie". Christophe Boudry is a fellow of "**Ministère de l'Enseignement Supérieur et de la Recherche**".

REFERENCES

Boudry C. Classification cellulaire par morphologie mathématique. (1997), Thèse de Doctorat of the University of Caen.

Coster M, Chermant JL. Precis d'analyse d'images (1985), Les Editions du CNRS.

Coster M, Chermant JL. Precis d'analyse d'images (1989), 2nd Edition: Les Presses du CNRS.

Duigou F, Galle I, Herlin P, Mandard AM. Improvement in slide preparation from archival material for automated DNA measurement by image analysis. Anal Quant Cytol Histol 1997; **19**: 167-73.

Feulgen R, Rossenbeck H. Mikroskopich chemischer nacheis einer nucleinsaure von typus der thymonuckleinsaure und die darauf beruhende elektive farbunf von zellkernen in mikroskopichen praparaten. Z Physiol Chem 1924; **135**: 203-24.

Serra J. Image Analysis and Mathematical Morphology. Academic Press, London, 1982.

Serra J. Image Analysis and Mathematical Morphology. Vol II. Theoretical Advances. Academic Press, 1988.

Van Driel KulkerAMJ, Mesker WE, Van der Burg MJM, Ploem JS. Preparation of cells from paraffin-embedded tissue for cytometry and cytomorphologic evaluation. Anal Cell Pathol 1987; **9**: 225-31.